Published in final edited form as:

J Biomed Mater Res B Appl Biomater. 2018 July ; 106(5): 1858–1868. doi:10.1002/jbm.b.33997.

Laser micro-ablation of fibrocartilage tissue: effects of tissue processing on porosity modification and mechanics

AM Matuska[1] and **PS McFetridge**[1,*]

[1]J. Crayton Pruitt Family Department of Biomedical Engineering, University of Florida, Biomedical Science Building JG56, P.O. Box 116131, 1275 Center Drive, Gainesville, FL 32611-6131, USA

Abstract

The temporomandibular joint disc (TMJ*d*) is an extremely dense and avascular fibrocartilaginous extracellular matrix (ECM) resulting in a limited regenerative capacity. The use of decellularized TMJ*d* as a biocompatible scaffold to guide tissue regeneration is restricted by innate subcellular porosity of the ECM that hinders cellular infiltration and regenerative events. Incorporation of an artificial microporosity via laser micro-ablation (LMA) can alleviate these cell and diffusion based limitations. In this study, LMA was performed either before or after decellularization to assess to effect of surfactant treatment on porosity modification as well as the resultant mechanical and physical scaffold properties. Under convective flow or agitation schemes, pristine and laser ablated discs were decellularized using either low (0.1% w/v) or high (1% w/v) concentrations of sodium dodecyl sulfate (SDS). Results show that lower concentrations of SDS minimized collagen degradation and tissue swelling while retaining its capacity to solubilize cellular content. Regardless of processing scheme, laser ablated channels incorporated after SDS treatment were relatively smaller and more uniform than those incorporated before SDS treatment, indicating an altered laser interaction with surfactant treated tissues. Smaller channels correlated with less disruption of native biomechanical properties indicating surfactant pre-treatment is an important consideration when using laser micro-ablation to produce artificial porosity in *ex vivo* derived tissues.

Keywords

fibrocartilage; laser ablation; decellularization; porosity; regenerative medicine

INTRODUCTION

The temporomandibular joint disc (TMJ*d*) is a mechanically and structurally complex fibrocartilage tissue that supports rotation and translation of the jaw during normal function. Due to the intrinsic lack of repair in cartilaginous tissues following injury or disease, tissue engineering to regenerate or repair these tissues *de novo* is a promising approach [1,2]. Naturally derived tissues used as scaffolding materials offer unique advantages over synthetic materials due to intrinsic structural properties and the presence of bioactive molecules within the extracellular matrix (ECM) that facilitates cell-ECM interactions and

*Corresponding Author: Fax - (352) 373 9221, pmcfetridge@bme.ufl.edu.

direct tissue specific cellular remodeling[3–5]. As such, a regenerative strategy that utilizes a scaffold derived from a native TMJ*d* with bulk properties specific to this complex joint to guide and support cellular regeneration would be highly advantageous compared to less structured materials. The use of these materials requires a degree of processing to remove existing cells and soluble components that would otherwise elicit an overt foreign body response. This has been a successful strategy with a variety of tissues [6–10], and has more recently been applied to articular and fibrocartilages[11–15]. In addition to immune acceptance, it is important that the processing method minimizes ECM disruption in order to maintain the tissues original mechanical properties such that it can withstand mechanical loading, particularly during early remodeling [16,17].

Previous work preparing a porcine TMJ*d* scaffold compared the effects of commonly used decellularization agents sodium dodecyl sulfate (SDS), Triton X-100 and acetone/ethanol[12]. Results demonstrated that treatment with 1% SDS maintained disc compressive mechanical properties most similar to the native disc and preserved general structural morphology. While treatments can be tissue specific, SDS, an anionic surfactant, which works by disrupting protein-protein interactions and solubilizing cellular components, has been shown to be more effective at solubilizing cell membranes compared to non-ionic, zwitterionic, or hypo/hypertonic treatments[18,19]. In order to maintain the tissue's intrinsic structural and chemical properties, these aggressive treatments ideally should use the minimal effective dose to remove immunogenic epitopes; with the literature reporting a wide range of SDS concentrations (0.03%–2% w/v) in various decellularization protocols[18,20–25]. To reduce scaffold exposure to aggressive decellularization agents, dynamic methods such as agitation and convective flow have been employed to improve extraction efficiency [8].

Nutrient transport limitations and subcellular porosity within dense ECM inhibits cellular migration and integration[9,26,27]. A CO_2 laser ablation technique (termed laser micro-ablation or LMA) has been previously used to generate artificial microporosity within porcine TMJ*d* discs and shown to improve recellularization of these scaffolds[28]. Therefore, the purpose of this study was to further assess the LMA technique in relation to the decellularization process and evaluate the effect of surfactant treatment on porosity incorporation and the resultant mechanical and physical properties of TMJ*d* scaffolds. LMA was performed before or after discs were decellularized using two SDS concentrations (0.1% and 1%) delivered via two different methods (convective flow and agitation).

METHODS

Tissue isolation and laser micro-ablation

Porcine temporomandibular joints were obtained from 6–9 month old animals (IACUC # 201207534, Animal Technologies, Tyler, TX). The fibrocartilage discs were dissected by separating the mandible from the temporal bone and severing connections of the disc with surrounding structures. Following dissection of the disc and washing in phosphate-buffered saline (PBS), whole discs were frozen to −80°C. Half were lyophilized and laser micro-ablated (LMA) before decellularization and half were reserved to be lyophilized and LMA after. Prior to LMA, tissues were lyophilized for 24 hours (Millrock Technology, Kingston, NJ). Pores were ablated using a 40W CO_2 laser engraver (Hurricane Lasers, Las Vegas, NV)

with 0.2 second pulse duration (57.6 mJ) and a 1000 μm centerline separation. This pulse duration was necessary to produce full thickness pores as determined in preliminary testing. To obtain consistently sized scaffolds, 2–3 six mm diameter circular punches were removed from the intermediate regions of the whole TMJ discs, using a disposable biopsy punch (Miltex, York PA).

Decellularization schemes

Overall there were a total of 8 treatment groups assessed (Figure 1). The two main test groups were whether the scaffold had been LMA before or after decellularization. These groups were evaluated at two different SDS concentrations (1% and 0.1% SDS) with two methods of fluid delivery (convective flow or rotary agitation). These concentrations were chosen because preliminary studies demonstrated that SDS concentrations between 0.1% and 1% in culture media significantly reduced cell number and viability to near zero indicating complete cell solubilization (data not shown). The convective flow circuit (Figure 2) was driven by a peristaltic pump (Masterflex L/S, model 07551–10; Cole Parmer, Vernon Hills, IL) and consisted of an SDS reservoir (250 ml capacity bottle), and one way check valve with a cracking pressure of 1 psi (SMC, Yorba Linda, CA) to prevent back-flow. SDS solution (200 ml total) was continuously circulated at an average flow rate of 1 ml/min with a pulse frequency of 1.5 pulse/min for 72 hours, except when paused to take daily measurements and collect SDS solution aliquots. The system was designed to allow flow around the samples because of the small sample size and to prevent excessive pressure buildup. Pressure was monitored upstream of the samples with a digital pressure gage (Ashcroft, Stratford, CT) inserted at a 3 way valve. Average pressure within the LMA (before) disc circuit was approximately 50 psi, and in the LMA (after) circuit approximately 200 psi. Each convective flow circuit held three scaffolds in series, therefore, for each test condition a total of three independent systems had to be used to achieve the final n=9 scaffolds. In order to minimize variables between convective flow and rotary agitation, including the volume of surfactant to tissue, rotary agitation decellularization was also performed with three scaffolds per bottle and incubated in 200 mL of either a 0.1% or 1% SDS solution in 500 ml capacity bottles. Samples were continuously agitated on an orbital shaker at 100 rpm for 72 hours. Daily measurements and aliquots of the decellularization solution obtained as described in the following section.

Morphology of tissue and ECM degradation over time

Initially and at 24, 48, and 72 hours during the decellularization, scaffold thickness and photographs were obtained. At each time point, 15 ml of the decellularization solution from each system was also collected for analysis and replaced with fresh solution. DNA was assessed in solutions using PicoGreen assay following manufacturer's instructions (Life Technologies). As a marker of ECM degradation, hydroxyproline, was quantified in the decellularization solutions[29]. Briefly, solutions were hydrolyzed in 6N HCl for 24 hours at 60°C. Samples were neutralized with equimolar NaOH, oxidized with chloramine T (Fisher Scientific, Pittsburgh PA) and the chromophore produced by reaction with p-dimethylaminobenzaldehyde (Mallinckrodt Chemicals, St Louis, MO) was measured at 550 nm and compared to standards produced with trans-4-hydroxy-L-proline (Sigma Aldrich, St

Louis, MO). Values were converted to collagen assuming hydroxyproline content of collagen to be 13.5% [30].

Mechanical analysis

Following the 72 hour decellularization, non-LMA discs were then laser micro-ablated as described previously. Discs were hydrated and equilibrated in PBS at 37°C for 1 hour before bulk compressive mechanical testing (n=9). Specimens were placed in a hydrated testing chamber in a Biomomentum Mach-1 micromechanical system (Biomomentum Inc, Laval, Quebec, Canada). Samples were subject to unconfined compression under 20% deformation (strain) relative to original sample thickness for 15 cycles. This deformation was chosen based on MRI imaging and finite element modeling that shows change in disc thickness (compressive strain) at 15–20% while pathologic conditions such as bruxism can impart compressive strains up to 30%[31,32]. Deformation was defined as $\varepsilon=\Delta L/L_0$ with ΔL the change in sample thickness relative to L_0, the original samples thickness. An initial find contact of the platen at 0.05N was used to reset the displacement followed by a find contact of the sample at 0.05N. The difference in location was used to determine initial sample thickness (L_0) from which sinusoidal compression was programmed for each sample following $\varepsilon = \Delta\varepsilon \sin(\omega t)$, where $\Delta\varepsilon$ and ω are the respective deformation and frequency (20%, 0.5 Hz). The resulting stress was defined as $\sigma=F/A$ with F being compressive force and A being the cross sectional area of the disc. The steady state hysteresis curves were averaged for the last 5 cycles. An apparent compressive modulus (E) was derived from the slope of the average loading curve between 14–19% deformation ($E=\sigma/\varepsilon$). Slope was derived from the least-squares linear regression on the discrete stress/deformation data points within the specified interval. Hysteresis was calculated from the area between the loading and unloading curves and the peak stress of the steady state hysteresis cycles are also reported.

Analysis of ECM void fraction and laser ablated channel diameter

Following mechanical testing, tissues were embedded in Neg50 media (Richard Allen Scientific) and progressive transverse (n=4 randomly assigned samples) or coronal (n=4 randomly assigned samples) 10μm sections were obtained with a HM 550 cryostat (ThermoFisher Scientific, Waltham. MA). Sections were stained with standard hematoxylin & eosin, mounted, and images were acquired with an Axiocam ICc.1 at 5x objective magnification on an AxioObserver Microscope (Carl Zeiss, Jena, Germany). Coronal sections were used to evaluate void volume (n=3 images per scaffold). Relative areas of ECM and void space were quantified in three random fields of view and averaged using thresholding in ImageJ (NIH, Bethesda, MD). From this void percent was determined by $1-(A_{ECM}/A_{total})*100\%$, where A_{ECM} is the area covered by ECM, and A_{total} is the total are of the field analyzed. Transverse sections from the top, middle, and bottom regions were used to evaluate ablation hole diameter (n=3 images per region). The ablated area was determined with the Axiovision measurement tool, and converted to a diameter assuming circular geometry. While it is possible that the mechanical testing performed prior to sectioning may have impacted measurements obtained, all sample groups were tested under compression so relative comparisons between treatment groups are made.

Evaluation of laser micro-ablation geometry pre-and post-SDS treatment

In order to further investigate the effect of SDS treatment on LMA size and geometry, a separate cohort of native and decellularized discs (via 1% SDS, agitation) were lyophilized and laser micro-ablated using a range of pulse durations (0.3, 0.25, 0.2, 0.15, 0.1, 0.05; resulting energies 86.4, 72.0, 57.6, 43.2, 28.8, 14.4 mJ) with a 1000 μm centerline separation. Four images were acquired from the top, middle, and bottom regions of ablated pores (total of n=12). Ablation diameter was measured within the Axiovision software as described in the previous section. Scanning electron microscopy (SEM) was performed to evaluate the cross sectional geometry of the ablated channels obtained from a 0.2 sec pulse duration. Freeze dried samples were CO_2 critical point dried (Autosamdri-815, Tousimis, Rockville, MD) and palladium gold sputtered (DeskV, Denton Vacuum, Moorestown, NJ). Images were collected using a Hitachi S-4000 FESEM at 10 kV at 30x magnification.

Statistical analysis

Mean and standard deviation were determined for all samples (n=3–9). A full factorial three factor ANOVA was used to determine the significant main and interaction effects of decellularization method, SDS concentration, and sequence of LMA (α=0.05). When significance was indicated and post hoc was necessary, Fisher's LSD with a Bonferroni correction was performed.

RESULTS

Morphological Outcomes

At 24, 48, and 72 hours during the course of the decellularization, tissue thickness (Figure 3) was significantly greater in samples subject to orbital agitation compared to samples exposed to convective flow ($p=0.001$, $p<0.001$, $p<0.001$, respectively). Swelling was also observed in samples incubated with 1% SDS compared to both 0.1% SDS at all time points ($p<0.001$). Whether LMA was performed before decellularization did not affect tissue ending thickness ($p=0.185$, $p=0.643$, $p=0.734$). Average initial thickness of all scaffolds was 2.1 ± 0.3 mm. There was a 5–17% increase (swelling) in tissue thickness under agitation compared to an 8% and 2% decrease (tissue compaction) in sample thickness from convective flow.

DNA Solubilization and Collagen Degradation

At all time points, DNA solubilization was greater in tissues that had been LMA (before SDS) compared to those that were not (Figure 4, $p=0.035$, $p=0.003$, $p=0.006$). Assessment of collagen dissociation from the tissue (Figure 4) showed a significantly greater release of solubilized collagen from tissue that was LMA (before SDS) compared to LMA (after SDS) tissue at all time points ($p<0.001$). After 72 hours, LMA (before SDS) tissues had released between 1.1±0.6% and 3.5±0.9% (mg collagen/mg scaffold) whereas LMA (after SDS) tissues had only released between 0.3±0.1% and 0.6±0.1% (mg collagen/mg scaffold). By 72 hours, there was also significantly greater collagen loss when using high concentrations of SDS compared to low concentrations ($p=0.036$). A two-way interaction showed that when

tissue had been LMA (before SDS), agitation resulted in greater collagen loss than convective flow (p=0.043).

Mechanical Evaluation

As expected from viscoelastic materials, decellularized discs displayed characteristic hysteresis profiles when subjected to 20% compressive deformation relative to the initial thickness (Figure 5). The apparent compressive moduli, derived from the steady state loading curves of the hysteresis loops, showed that samples which were not LMA until after SDS treatment were stiffer than those that were LMA before SDS treatment (p<0.001). Compressive modulus values were 1.3 to 2.2x higher in scaffolds that were LMA after SDS treatment. Neither SDS concentration (p=0.932) or method of decellularization (p=0.571) affected modulus values. Since sample thickness varied based on treatment method, initial thickness of the sample is an important consideration when interpreting the mechanical results. Mechanically derived thickness values showed the largest difference in actual sample thickness was between convective flow and agitation groups. Convective flow sample thicknesses were 2.2 ±0.2 (0.1% LMA after), 2.1 ± 0.2 (1% LMA after), 2.1 ±0.3 (0.1% LMA before), and 2.1 ± (1% LMA before). Agitation sample thicknesses were 2.5 ±0.1 (0.1% LMA after), 2.4 ±0.2 (1% LMA after), 2.5 ±0.2 (0.1% LMA before), and 2.5±0.3 (1% LMA before) which maintained an aspect ratio between 0.35–0.42 for all samples tested.

Average hysteresis values determined from steady state hysteresis loops was significantly greater in discs that were LMA after SDS treatment compared to those that were LMA before SDS (Figure 6A, p=0.001). When LMA was performed after SDS treatment, 1.4 to 2.2x higher peak stresses were also attained compared to when LMA was performed before SDS treatment (Figure 6B, p<0.001).

ECM Evaluation

H&E staining demonstrated all the decellularization strategies effectively solubilized visible cells from TMJd scaffolds. Void fraction within the ECM was quantified from histological sections at the termination of all processing steps. Samples decellularized by agitation had higher void fractions (15–20%) than those decellularized by convective flow (5–10%), (Figure 7, p<0.001). The sequence of LMA (p=0.109) and the concentration of SDS (p=0.987) did not influence the measured void fraction.

Laser Micro-Ablation Geometry

The average diameter of the laser ablated channels was smaller and more uniform when samples were treated with SDS before LMA (Figure 8, p<0.001). Diameters ranged from 240–295 μm with a standard deviation between 54 and 64 μm (295 ± 60, 259 ± 60, 240 ± 54, and 257 ± 64). This is compared to samples which were LMA before SDS treatment where channel diameter ranged from 455–489 μm with standard deviation between 72–122 μm (455 ± 73, 487 ± 122, 480 ±113, and 490 ± 110). A three way interaction between SDS concentration, delivery method, and LMA sequence was detected (p=0.005). When LMA is performed after SDS treatment, channel diameter was significantly larger when low concentration of SDS was used under convective flow (p<0.005).

To further investigate this overall phenomenon a new set of samples were prepared, and channel diameters were assessed over a range of pulse durations, on decellularized (1% agitation) and native discs. Ablation diameter was consistently smaller on discs that had been previously treated with SDS over the entire range of pulse durations tested (Figure 9, $p<0.001$). Extended pulse durations (0.2 sec) were required to ablate through the full thickness of the native disc compared to decellularized discs (0.1 sec). This translates to a much larger channel diameter to achieve the same depth in native tissue (425 μm) compared to in decellularized tissue (200 μm). There were also obvious differences in the geometry and uniformity of the ablated channels evidenced by SEM (Figure 9). In LMA (before SDS) discs, channels were irregular with a diameter that was larger at the top surface, tapering to a small point at the bottom, whereas in LMA (after SDS) discs, channels were smooth with very little diameter variation.

DISCUSSION

The purpose of this study was to determine the interaction of surfactant-based decellularization on laser micro-ablation of an *ex-vivo* derived TMJ fibrocartilage scaffold with a specific focus on mechanical and morphological outcomes. Due to the joint's complex loading physiology it is essential that the structural integrity of the replacement disc be maintained as much as possible to ensure continued function. Further, early cellular remodeling events are guided by ECM morphology and can significantly influence outcomes of cellular integration and function.

Surfactant chemistry suggests that detergents are effective at the critical micelle concentration (CMC). For SDS this ranges from 8.5 mM to 3.5 mM with a 0.1% w/v solution of SDS approximately 3.5 mM[33]. In these investigations, results have shown that both SDS concentrations (0.1% and 1%), and agitation or perfusion schemes, were effective at solubilizing whole cells from the TMJ scaffolds. The use of low SDS concentrations is desirable as it reduces the potential of cytotoxic effects that may result from residual surfactant, and reduces ionic denaturation of the ECM proteins. Hudson *et al*[34] evaluated the effects of amphoteric, anionic, cationic, non-ionic detergents at their CMC and 10x CMC on nerve decellularization and showed anionic and amphoteric detergents to be more effective in terms of cell removal and morphological preservation. Amphoteric detergents were more effective at high concentrations, while anionic detergents, like SDS, were more effective at low concentrations. The authors attribute this to packing density of the micelles, which is limited in charged anionic surfactants due to head group repulsion. Other studies confirm the effectiveness of SDS at concentrations between 0.075% and 0.1%[15,35]. Specifically Stapleton *et al* showed that lower concentrations (0.1% [w/v]) did not damage the tissue ECM while still effectively removing cellular components in meniscus tissue decellularization.

During heart valve decellularization, collagen loss has been shown to increase proportionally with incubation time[36]. Investigations herein show increased collagen degradation over decellularization time and at 1% SDS compared to 0.1%. A higher concentration of collagen was lost with LMA tissues (before SDS), likely due to fragmentation of collagen fibers by the LMA process resulting in additional deterioration. Fragmentation and swelling of

collagen has been noted in tissues decellularized with high concentrations of SDS[37]. The results are consistent with previous studies showing bulk swelling of the scaffold irrespective of the sequence of laser micro ablation (before or after) decellularization. Swelling effects were more pronounced in scaffolds treated with 1% SDS verses 0.1% SDS. This was minimized in convective flow due to higher pressures in the convective flow circuit which likely acted to compact the scaffold. The assessment of microscopic void space on histologic sections demonstrated no significant difference between 0.1% and 1% SDS treatments but did between convective flow and agitation.

Several studies have investigated the effect of pressure in decellularization strategies[8,38,39]. High hydrostatic pressure in the range of 1 GPa resulted in compaction and ineffective removal of nuclei in aortic tissue compared to SDS decellularization[38], yet another study noted that periodic pressurization with enzymatic treatments was more effective than strategies without an applied pressure gradient when decellularizing porcine dermis[39]. Montoya *et al* demonstrated differential extraction efficiency of phospholipid and protein from the human umbilical vein depending on the pressure used. High pressure (150 mmHg) more efficiently extracted phospholipid, while low pressure (50 mmHg) more efficiently extracted protein[8]. It has also been noted that pressure must be carefully monitored in perfusion decellularization of whole organs, to ensure the vasculature and other fine structures remain intact[40,41]. Lower concentration of SDS used in these decellularization protocols resulted in less collagen degradation and ECM alteration, however optimum concentration may vary by the delivery method. For example, higher concentrations of SDS may be necessary when pressure based decellularization is used, as ECM compaction reduces permeability and thus SDS-tissue interactions.

No effects on bulk tissue mechanics were noted between either 0.1% or 1% SDS treatments, however the sequence of LMA (either before or after SDS) affected the scaffolds' mechanical properties significantly. Scaffolds LMA after SDS treatment displayed increased compressive modulus, hysteresis, and peak stress. These outcomes could result from a combination of the increased degradation of collagen observed in LMA tissues and from differences in CO_2 laser ablation geometry, namely smaller channel diameter, when LMA was performed after decellularization[42–44].

The process of tissue ablation occurs in a cycle. As the laser light interacts with the tissue, heat is generated as photons are absorbed, leading to an increase in temperature, and finally ablation once the tissue reaches a threshold temperature[45]. For example, the main chromophore in the IR range is water which dominates the absorption properties of tissues [46,47]. This necessitates freeze drying prior to laser ablation to reduce initial incident light scattering as determined previously[28]. The geometry of ablated tissue is therefore dictated by initial absorption/scattering characteristics and subsequent heat transfer (thermal diffusion) resulting from thermodynamic properties of the tissue[48]. Native tissue is heterogeneous with many different components such as cell membranes, DNA/RNA, collagen, glycosaminoglycans, and water. The density and abundance of potential scattering molecules in the ECM likely decreased as a result of SDS treatment. This would lead to a more rapid increase in localized temperature given the same CO_2 pulse resulting in smaller channel diameter. The difference observed in laser ablation between native and

decellularized TMJd fibrocartilage also indicates the difference that may be observed for other tissue types based on heat transfer properties of the tissue.

The wavelength of a CO_2 laser (10.2 μm) dictates the smallest spot size a beam could be focused to, meaning realistic ablation diameters are more likely to be a few hundred microns [49]. The energy delivered by a continuous CO_2 laser is proportional to duration of the pulse, therefore pulse duration will also impact channel depth and diameter to some extent. We were able to demonstrate that the average channel diameter was consistently smaller over a range of pulse durations in samples which had been SDS-treated first. A pulse duration of 0.1 s resulted in a continuous pore through the thickness of a decellularized disc with average diameter of 205 μm. The same pulse duration on non-decellularized discs, produced a pore diameter of 340 μm and failed to penetrate through the scaffold. By extending the pulse duration to 0.2 s a continuous pore was created however the diameter was significantly larger at 425 μm. Pore sizes within various tissue engineering scaffolds has been studied and it has been found that optimal pore size which supports cell migration and ingrowth is between 100–325 μm [28,50,51].

In conclusion, it was demonstrated that LMA parameters such as pulse duration can be altered to produce channels with a range of diameters (120–300+ μm) within previously decellularized scaffolds. Future work is needed to determine optimum cell reseeding methods in conjunction with pore size, pattern, and culture regimes to further improve cellular integration and enhance remodeling. While the less porous geometry observed in convective flow decellularized tissue is more similar to native structures; it is likely that the increased porosity of the bulk ECM from agitation based decellularization may improve initial cellular integration into the ECM itself. Agitation decellularization may also offer benefits in scaled processes where a higher throughput can be achieved. Lastly, in agitation based decellularization, lower concentrations of SDS can be used that minimizes ECM degradation, preserve general morphology and reduces the risk of residual surfactant contamination in the scaffold.

Acknowledgments

The authors would like to thank Cassandra Juran and Aurore van de Walle for assistance in collection of scanning electron microscopy images. We gratefully acknowledge the support of the National Institute of Dental and Craniofacial Research at the US National Institutes of Health (NIH; 1R21DE022449) and the National Science Foundation Graduate Research Fellowship (DGE-1315138). Any opinion, findings, and conclusions or recommendations expressed in this material are those of the authors and do not necessarily reflect the views of the National Institutes of Health or National Science Foundation.

References

1. Chung C, Burdick JA. Engineering cartilage tissue. Adv Drug Deliv Rev. 2008; 60(2):243–62. [PubMed: 17976858]
2. Laurencin CT, Ambrosio AM, Borden MD, Cooper JA Jr. Tissue engineering: orthopedic applications. Annu Rev Biomed Eng. 1999; 1:19–46. [PubMed: 11701481]
3. Stevens MM, George JH. Exploring and engineering the cell surface interface. Science. 2005; 310(5751):1135–8. [PubMed: 16293749]
4. Benders KE, van Weeren PR, Badylak SF, Saris DB, Dhert WJ, Malda J. Extracellular matrix scaffolds for cartilage and bone regeneration. Trends Biotechnol. 2013; 31(3):169–76. [PubMed: 23298610]

5. Uzarski JS, Van De Walle AB, McFetridge PS. Preimplantation processing of ex vivo-derived vascular biomaterials: effects on peripheral cell adhesion. J Biomed Mater Res A. 2013; 101(1): 123–31. [PubMed: 22825780]
6. Goktas S, Pierre N, Abe K, Dmytryk J, McFetridge PS. Cellular interactions and biomechanical properties of a unique vascular-derived scaffold for periodontal tissue regeneration. Tissue Eng Part A. 2010; 16(3):769–80. [PubMed: 19778172]
7. McFetridge PS, Daniel JW, Bodamyali T, Horrocks M, Chaudhuri JB. Preparation of porcine carotid arteries for vascular tissue engineering applications. J Biomed Mater Res A. 2004; 70(2):224–34. [PubMed: 15227667]
8. Montoya CV, McFetridge PS. Preparation of ex vivo-based biomaterials using convective flow decellularization. Tissue Eng Part C Methods. 2009; 15(2):191–200. [PubMed: 19196128]
9. Moore M, Sarntinoranont M, McFetridge P. Mass transfer trends occurring in engineered ex vivo tissue scaffolds. J Biomed Mater Res A. 2012; 100(8):2194–203. [PubMed: 22623220]
10. Sullivan DC, Mirmalek-Sani SH, Deegan DB, Baptista PM, Aboushwareb T, Atala A, Yoo JJ. Decellularization methods of porcine kidneys for whole organ engineering using a high-throughput system. Biomaterials. 2012; 33(31):7756–64. [PubMed: 22841923]
11. Elder BD, Eleswarapu SV, Athanasiou KA. Extraction techniques for the decellularization of tissue engineered articular cartilage constructs. Biomaterials. 2009; 30(22):3749–56. [PubMed: 19395023]
12. Lumpkins SB, Pierre N, McFetridge PS. A mechanical evaluation of three decellularization methods in the design of a xenogeneic scaffold for tissue engineering the temporomandibular joint disc. Acta Biomater. 2008; 4(4):808–16. [PubMed: 18314000]
13. Schwarz S, Koerber L, Elsaesser AF, Goldberg-Bockhorn E, Seitz AM, Durselen L, Ignatius A, Walther P, Breiter R, Rotter N. Decellularized cartilage matrix as a novel biomatrix for cartilage tissue-engineering applications. Tissue Eng Part A. 2012; 18(21–22):2195–209. [PubMed: 22690787]
14. Zang M, Zhang Q, Chang EI, Mathur AB, Yu P. Decellularized tracheal matrix scaffold for tissue engineering. Plast Reconstr Surg. 2012; 130(3):532–40. [PubMed: 22929238]
15. Stapleton TW, Ingram J, Katta J, Knight R, Korossis S, Fisher J, Ingham E. Development and characterization of an acellular porcine medial meniscus for use in tissue engineering. Tissue Eng Part A. 2008; 14(4):505–18. [PubMed: 18370607]
16. Goktas S, Matuska AM, Pierre N, Gibson TM, Dmytryk JJ, McFetridge PS. Decellularization method influences early remodeling of an allogenic tissue scaffold. J Biomed Mater Res A. 2013
17. Matuska AM, McFetridge PS. The effect of terminal sterilization on structural and biophysical properties of a decellularized collagen-based scaffold; implications for stem cell adhesion. J Biomed Mater Res B Appl Biomater. 2014
18. Oberwallner B, Brodarac A, Choi YH, Saric T, Anic P, Morawietz L, Stamm C. Preparation of cardiac extracellular matrix scaffolds by decellularization of human myocardium. J Biomed Mater Res A. 2013
19. Gilbert TW, Sellaro TL, Badylak SF. Decellularization of tissues and organs. Biomaterials. 2006; 27(19):3675–83. [PubMed: 16519932]
20. Faulk DM, Carruthers CA, Warner HJ, Kramer CR, Reing JE, Zhang L, D'Amore A, Badylak SF. The effect of detergents on the basement membrane complex of a biologic scaffold material. Acta Biomater. 2014; 10(1):183–93. [PubMed: 24055455]
21. Youngstrom DW, Barrett JG, Jose RR, Kaplan DL. Functional characterization of detergent-decellularized equine tendon extracellular matrix for tissue engineering applications. PLoS One. 2013; 8(5):e64151. [PubMed: 23724028]
22. Rieder E, Kasimir MT, Silberhumer G, Seebacher G, Wolner E, Simon P, Weigel G. Decellularization protocols of porcine heart valves differ importantly in efficiency of cell removal and susceptibility of the matrix to recellularization with human vascular cells. J Thorac Cardiovasc Surg. 2004; 127(2):399–405. [PubMed: 14762347]
23. Cebotari S, Tudorache I, Jaekel T, Hilfiker A, Dorfman S, Ternes W, Haverich A, Lichtenberg A. Detergent decellularization of heart valves for tissue engineering: toxicological effects of residual detergents on human endothelial cells. Artif Organs. 2010; 34(3):206–10. [PubMed: 20447045]

24. Amensag S, McFetridge PS. Rolling the human amnion to engineer laminated vascular tissues. Tissue Eng Part C Methods. 2012; 18(11):903–12. [PubMed: 22616610]
25. Lu Q, Ganesan K, Simionescu DT, Vyavahare NR. Novel porous aortic elastin and collagen scaffolds for tissue engineering. Biomaterials. 2004; 25(22):5227–37. [PubMed: 15110474]
26. Moore M, Moore R, McFetridge PS. Directed oxygen gradients initiate a robust early remodeling response in engineered vascular grafts. Tissue Eng Part A. 2013; 19(17–18):2005–13. [PubMed: 23541106]
27. Tosun Z, McFetridge PS. Improved recellularization of ex vivo vascular scaffolds using directed transport gradients to modulate ECM remodeling. Biotechnol Bioeng. 2013; 110(7):2035–45. [PubMed: 23613430]
28. Juran CM, Dolwick F, McFetridge PS. Engineered Microporosity: Enhancing the early regenerative potential of decellularized TMJ discs. Tissue Eng Part A. 2014
29. Creemers LB, Jansen DC, van Veen-Reurings A, van den Bos T, Everts V. Microassay for the assessment of low levels of hydroxyproline. Biotechniques. 1997; 22(4):656–8. [PubMed: 9105617]
30. Neuman RE, Logan MA. The determination of collagen and elastin in tissues. J Biol Chem. 1950; 186(2):549–56. [PubMed: 14794650]
31. Koolstra JH, van Eijden TM. Combined finite-element and rigid-body analysis of human jaw joint dynamics. J Biomech. 2005; 38(12):2431–9. [PubMed: 16214491]
32. Li Q, Ren S, Ge C, Sun H, Lu H, Duan Y, Rong Q. Effect of jaw opening on the stress pattern in a normal human articular disc: finite element analysis based on MRI images. Head Face Med. 2014; 10:24. [PubMed: 24943463]
33. Seddon AM, Curnow P, Booth PJ. Membrane proteins, lipids and detergents: not just a soap opera. Biochim Biophys Acta. 2004; 1666(1–2):105–17. [PubMed: 15519311]
34. Hudson TW, Liu SY, Schmidt CE. Engineering an improved acellular nerve graft via optimized chemical processing. Tissue Eng. 2004; 10(9–10):1346–58. [PubMed: 15588395]
35. Schaner, PJ., Martin, ND., Tulenko, TN., Shapiro, IM., Tarola, NA., Leichter, RF., Carabasi, RA., Dimuzio, PJ. J Vasc Surg. United States: 2004. Decellularized vein as a potential scaffold for vascular tissue engineering; p. 146-53.
36. Schenke-Layland K, Vasilevski O, Opitz F, Konig K, Riemann I, Halbhuber KJ, Wahlers T, Stock UA. Impact of decellularization of xenogeneic tissue on extracellular matrix integrity for tissue engineering of heart valves. J Struct Biol. 2003; 143(3):201–8. [PubMed: 14572475]
37. Bodnar E, Olsen EG, Florio R, Dobrin J. Damage of porcine aortic valve tissue caused by the surfactant sodiumdodecylsulphate. Thorac Cardiovasc Surg. 1986; 34(2):82–5. [PubMed: 2424134]
38. Eichhorn S, Baier D, Horst D, Schreiber U, Lahm H, Lange R, Krane M. Pressure shift freezing as potential alternative for generation of decellularized scaffolds. Int J Biomater. 2013; 2013:693793. [PubMed: 23818900]
39. Prasertsung I, Kanokpanont S, Bunaprasert T, Thanakit V, Damrongsakkul S. Development of acellular dermis from porcine skin using periodic pressurized technique. J Biomed Mater Res B Appl Biomater. 2008; 85(1):210–9. [PubMed: 17853423]
40. Badylak SF, Taylor D, Uygun K. Whole-organ tissue engineering: decellularization and recellularization of three-dimensional matrix scaffolds. Annu Rev Biomed Eng. 2011; 13:27–53. [PubMed: 21417722]
41. Arenas-Herrera JE, Ko IK, Atala A, Yoo JJ. Decellularization for whole organ bioengineering. Biomed Mater. 2013; 8(1):014106. [PubMed: 23353764]
42. Korhonen, RK., Laasanen, MS., Toyras, J., Lappalainen, R., Helminen, HJ., Jurvelin, JS. J Biomech. United States: 2003. Fibril reinforced poroelastic model predicts specifically mechanical behavior of normal, proteoglycan depleted and collagen degraded articular cartilage; p. 1373-9.
43. Olde Damink LH, Dijkstra PJ, Van Luyn MJ, Van Wachem PB, Nieuwenhuis P, Feijen J. Changes in the mechanical properties of dermal sheep collagen during in vitro degradation. J Biomed Mater Res. 1995; 29(2):139–47. [PubMed: 7738060]
44. Lakes EH, Matuska AM, McFetridge PS, Allen KD. Mechanical Integrity of a Decellularized and Laser Drilled Medial Meniscus. J Biomech Eng. 2016; 138(3)

45. LeCarpentier GL, Motamedi M, McMath LP, Rastegar S, Welch AJ. Continuous wave laser ablation of tissue: analysis of thermal and mechanical events. IEEE Trans Biomed Eng. 1993; 40(2):188–200. [PubMed: 8319970]

46. Jansen ED, Frenz M, Kadipasaoglu KA, Pfefer TJ, Altermatt HJ, Motamedi M, Welch AJ. Laser-tissue interaction during transmyocardial laser revascularization. Ann Thorac Surg. 1997; 63(3): 640–7. [PubMed: 9066377]

47. Vogel A, Venugopalan V. Mechanisms of pulsed laser ablation of biological tissues. Chem Rev. 2003; 103(2):577–644. [PubMed: 12580643]

48. Walsh JT Jr, Flotte TJ, Deutsch TF. Er:YAG laser ablation of tissue: effect of pulse duration and tissue type on thermal damage. Lasers Surg Med. 1989; 9(4):314–26. [PubMed: 2761327]

49. Welch AJ, Torres JH, Cheong WF. Laser physics and laser-tissue interaction. Tex Heart Inst J. 1989; 16(3):141–9. [PubMed: 15227198]

50. Cooper JA, Lu HH, Ko FK, Freeman JW, Laurencin CT. Fiber-based tissue-engineered scaffold for ligament replacement: design considerations and in vitro evaluation. Biomaterials. 2005; 26(13): 1523–32. [PubMed: 15522754]

51. Murphy, CM., Haugh, MG., O'Brien, FJ. Biomaterials. England: 2010. The effect of mean pore size on cell attachment, proliferation and migration in collagen-glycosaminoglycan scaffolds for bone tissue engineering; p. 461-6.

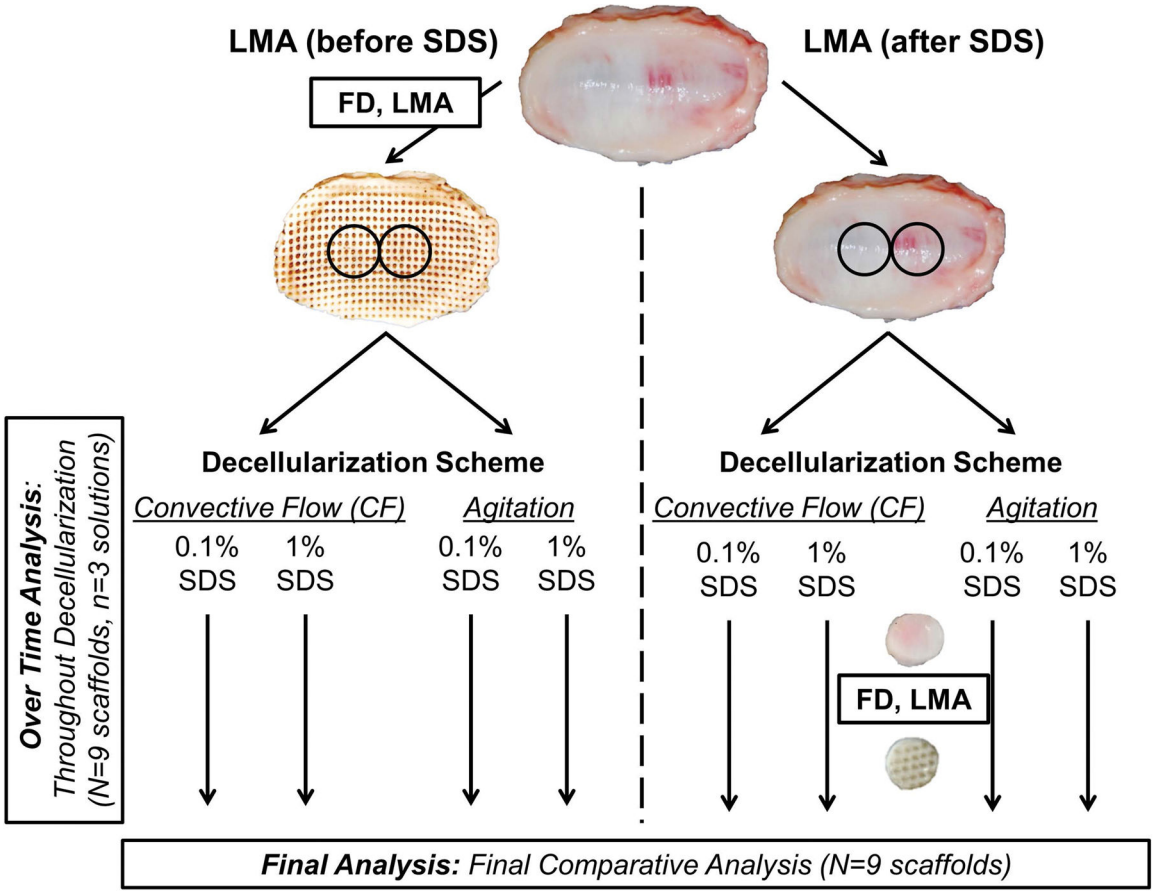

Figure 1.

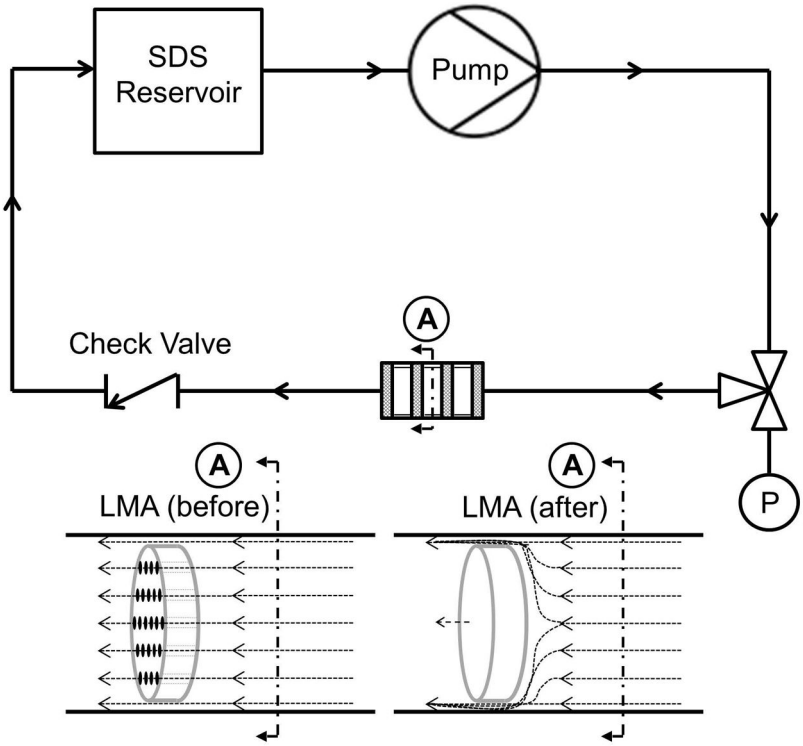

Figure 2.

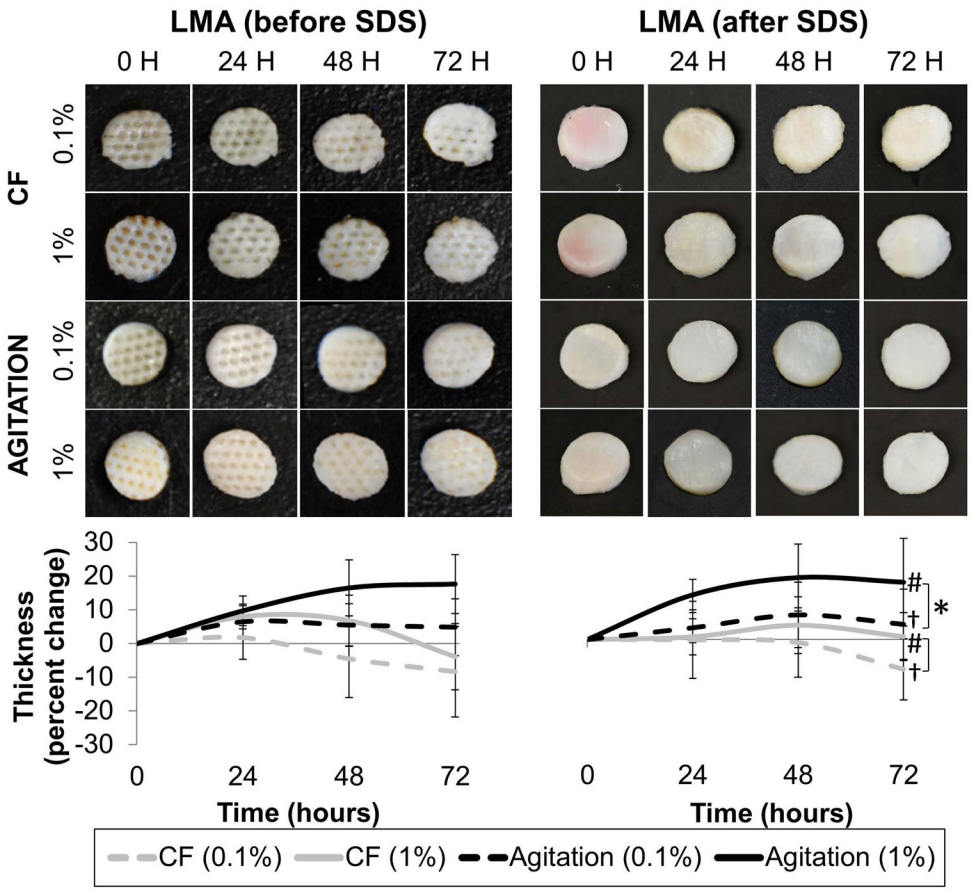

Figure 3.

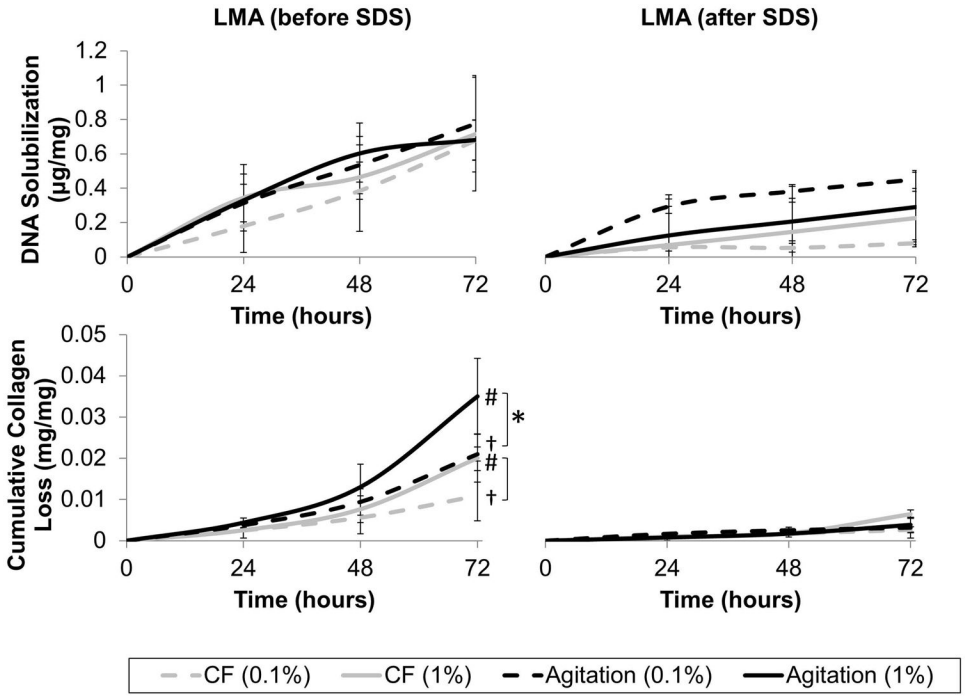

Figure 4.

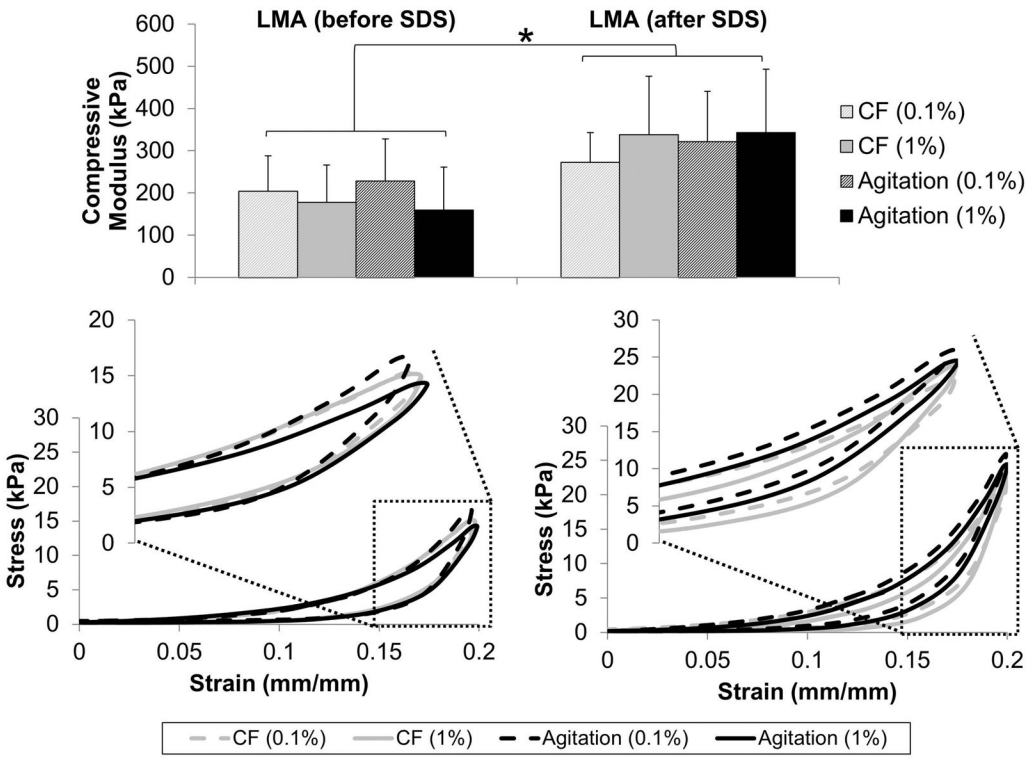

Figure 5.

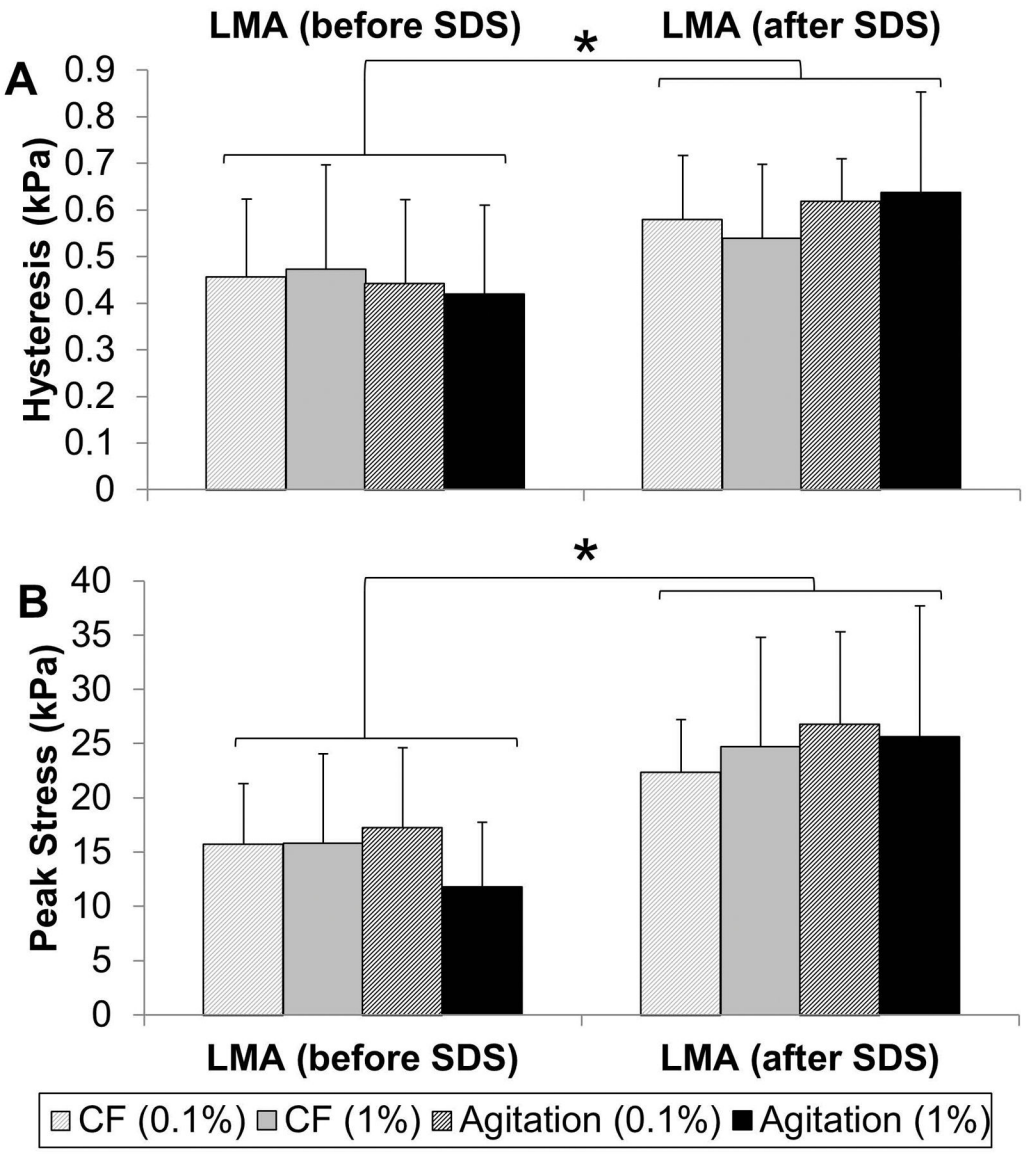

Figure 6.

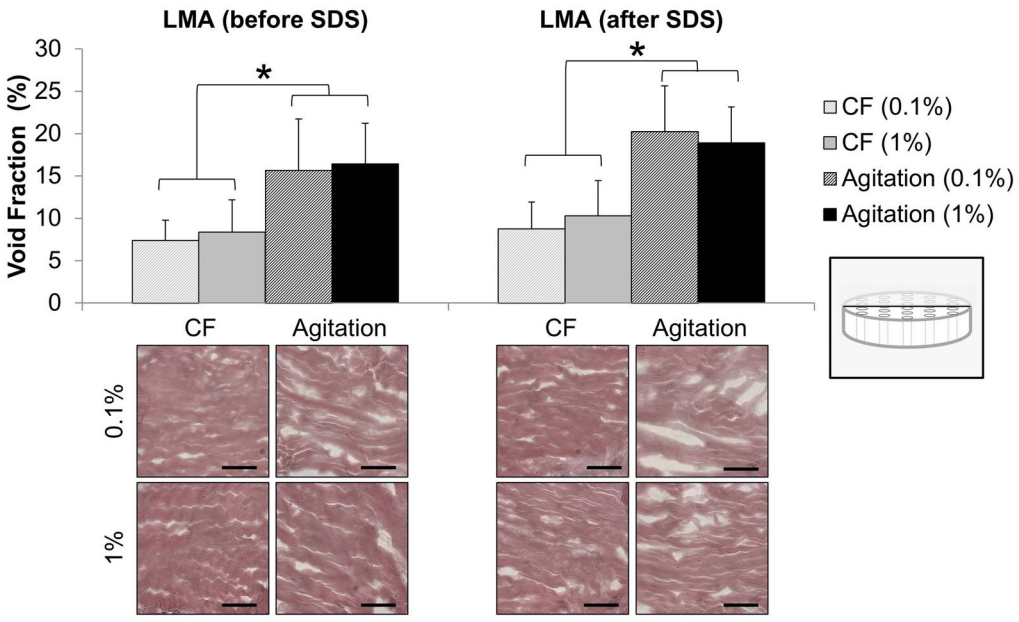

Figure 7.

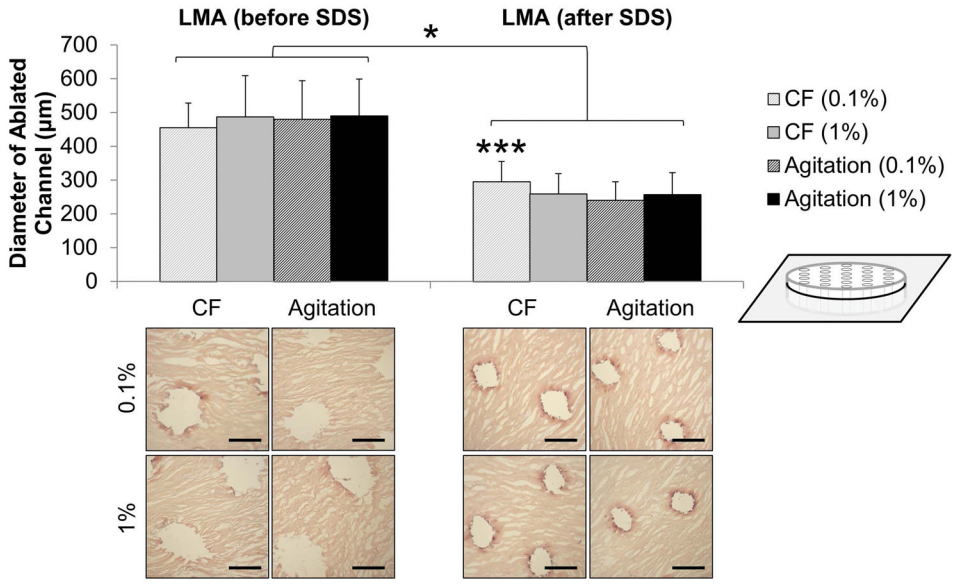

Figure 8.

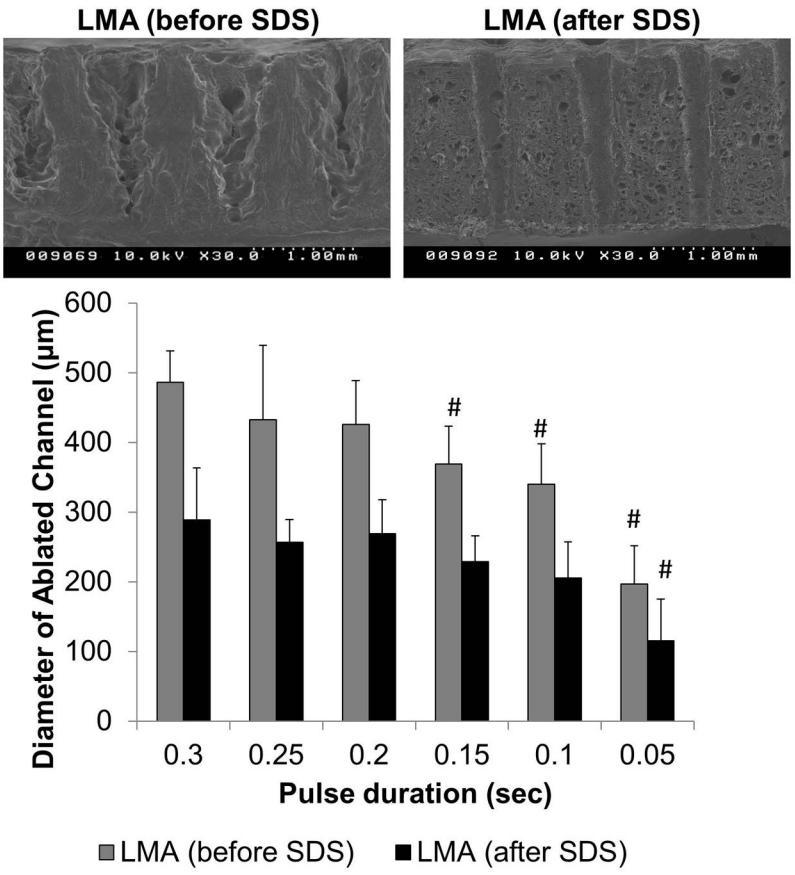

Figure 9.